Desalination and Water Treatment
www.deswater.com

doi: 10.5004/dwt.2021.26911

220 (2021) 342–352
April

Sequestration of crystal violet from aqueous solution using ash of black turmeric rhizome

Asha Patel[a], Sanju Soni[a], Jyoti Mittal[b], Alok Mittal[b], Charu Arora[a,*]

[a]*Department of Chemistry, Guru Ghasidas University, Bilaspur – 495009, Chhattisgarh, India, Tel. +91 758709551; emails: charuarora150@gmail.com/charu_arora@yahoo.com (C. Arora)*
[b]*Department of Chemistry, Maulana Azad National Institute of Technology, Bhopal, India*

Received 15 August 2020; Accepted 6 December 2020

ABSTRACT

Activated carbon obtained from rhizomes of black turmeric is used for the removal of industrial pollutant crystal violet dye from aqueous solution. The ash was characterized by Fourier transform infrared, X-ray diffraction (XRD), and scanning electron microscopy. Powder XRD pattern of the adsorbent reveals the peaks at 2θ angles 26.7°, 28.6°, 30.5°, 32.8°, 34.1°, 40.64°, 43.4°, and 45.1° and pattern was found to remain unchanged after every cycle (after desorption) till eighth cycles. The calculated column adsorption capacity lower than the batch adsorption capacity. IR peaks of black turmeric ash before adsorption were observed at 1,397.33 and 1,007.13 cm^{-1} and after adsorption it shifted to 1,012.62 cm^{-1}. Studies on effect of various parameters viz. dye concentration, dose of adsorbent, contact time, pH, and temperature were carried out. The dye adsorption increases with increasing pH and temperature. In higher pH ranges the adsorbent surface carries negative charge which benefits the adsorption of cationic crystal violet dye through electrostatic interaction. 100% dye removal was achieved at 40°C and above. Mechanism and kinetics of the adsorption process have also been investigated. Temkin adsorption isotherm was found best fit for adsorption process indicating the presence the energetically non-equivalent adsorption sites present on the surface of adsorbent and the adsorption of CV takes place on the more energetic adsorption site at first. Pseudo-second-order kinetics with rate constant 1.85×10^{-4} g/mg min is best fit for the adsorption process. Adsorption was found to be endothermic and processed via chemisorption.

Keywords: Crystal violet; Adsorption isotherms; Adsorption kinetics; Dye removal; Black turmeric

1. Introduction

Water is crucial for life. It is essential to save water to safeguard the earth as well as future of mankind. With development of science and technology and rapid industrialization, our world is touching new horizons but we are paying a high cost of it in form of widespread problem of environmental pollution. About 80% of world's wastewater is dumped to water bodies mostly without proper treatment. One of the important classes of water pollutants is organic dyes, being used in paper, textile, leather, plastic, food, cosmetics, and pharmaceutical industries. High concentration of dyes in water bodies stop the oxygenation capacity of the receiving water and cut of sun light thus upsetting the biological activity of aquatic life and photosynthesis process of aquatic plants such as algae. Polluting effects of these dyes is also due to their non-biodegradability, they keep on accumulating in aquatic animals and plants as well as in the sediments. Decomposition of dyes into pollutants in carcinogenic or mutagenic compounds causing allergies, skin irritation, or different tissue changes [1]. It is desired to eliminate the organic dyes from industrial effluents prior to throwing it to water bodies. It is difficult to treat dye containing wastewater due to diverse chemical nature of dyes. Treatments like chlorination cannot be used as it release mutagenic products even from less harmful dyes [2].

* Corresponding author.

Adsorption has been revealed to be one of the most effective and established treatment of wastewater in textile industry as it is an economically achievable process for dyes removal and decolorization of textile effluents. The process involves the transfer of soluble organic dyes from wastewater to the surface of the adsorbent which is solid and highly porous material. The adsorbent adsorbs each compound to be removed to its capacity and when it is "spent" should be replaced by fresh material. The spent adsorbent may be either regenerated or incinerated. The main factors which influence dye adsorption are: interaction between dye and adsorbent, surface area, and particle size of adsorbent, pH, temperature, and time duration of contact. The most commonly used adsorbent is activated carbon. The cationic mordant and acid dyes are removed with high removal rates [3], whereas dispersed, vat, direct, pigment, and reactive dyes are removed with moderate removal rates [4]. Besides adsorption, several methods viz. photochemical degradation, chemical oxidation, advanced oxidation process (AOP), biological degradation, coagulation, reverse osmosis, flotation, electrochemical treatment, etc., are also used for dye removal study [5–11]. However, adsorption is most advantageous due to its cost-effectiveness, efficiency, and reusability. Various adsorbents viz. agricultural waste, coal, wood, fly ash, activated carbon, clay, and other porous materials have been used for the adsorptive removal of dye from its aqueous solutions [12–26]. It is also well-known that during the combustion of biomass or biomass/coal blends, the large amounts of alkali metals and alkaline earth metals in biomass or coal can also result in severe ash-related problems [27–29].

Black turmeric (*Curcuma caesia*) belonging to family *Zingiberaceae*, is a perennial herb with bluish black rhizomes. *C. caesia* has been used by tribal communities for medicinal purpose viz. hemorrhoids, leprosy, asthma, epilepsy, fever, wound, vomiting, menstrual disorder, tumor, piles, aphrodisiac, inflammation, gonorrhoeal discharges, since ancient times [30]. Some plant species belonging to family *Zingiberaceae* are reported to act as adsorbent for adsorptive removal of dyes [31]. However, still there arises a great need to explore new low cost adsorbent materials with high adsorption capacity. In the present study, we have undertaken to explore the potential role of *C. caesia* ash for removal of crystal violet from wastewater. Crystal violet (molecular formula $C_{25}H_{30}N_3Cl$, molecular weight 407.98 g/mol) is a cationic dye used in several industries such as dyeing and textile, paper, ball point pen, leather, additives, cosmetics, and analytical chemistry/biochemistry. Structure of dye is shown in Fig. 1. It has carcinogenic and mutagenic effects in rodents. It is known to cause eye irritation, skin irritation, digestive tract irritation, permanent injury to cornea, and conjunctiva. The dye reduces to leuco moiety, leucocrystal violet in effluent, leading to environmental deterioration [32–35]. In our previous and latest research, for the first time, *C. caesia* ash was used for the efficient removal of malachite green dye from aqueous solution where batch and column adsorption studies of malachite green onto *C. caesia* ash were carried out. Adsorption capacity for column process is found to be 38.16 mg/g which is less than that of batch process. Value for change in Gibbs free energy is negative over the entire temperature range, indicating the process to be spontaneous. The adsorption process is endothermic. [47].

In the present investigation, *C. caesia* ash is prepared from rhizome and explored for adsorptive removal of crystal violet dye from aqueous solution. The aim of the present study is to find the optimum conditions for the removal of crystal violet. For this purpose effect of parameters viz. pH, initial dye concentration, dose, temperature, and contact time has been investigated. Two techniques batch [36–38] and column processes [39,40] have been applied to study dye removal by *C. caesia* ash.

2. Experimental section

2.1. Materials and characterization techniques

All chemicals and reagents used in the present work are commercially available and used without any further purification. Concentration of crystal violet (CV) dye solution during adsorption was estimated spectrophotometrically using Shimadzu (Kyoto, Japan) UV 1800 spectrophotometer with a 10 mm quartz cuvette by recording absorbance at 589 nm (λ_{max}). Stock solution of the dye (100 mg/L) was prepared in distilled water. All working solutions with desired dye concentration were prepared from the stock solution by successive dilution. Scanning electron microscopy (SEM) micrographs of the adsorbent before and after adsorption were recorded using Merlin VP compact (Carl ZEISS Germany make) having air lock chamber [41]. The IR spectrum of the adsorbent was carried out using Nicolet iS10, Thermo Fisher Scientific Instrument, Madison, USA, OMNIC 9, and TQ analysis software packages Fourier transform infrared (FTIR) spectrometer. Zeta potential of the adsorbent suspended in aqueous solution was determined using a zeta-sizer nano-ZS (Malvern) at room temperature. The characterization of the adsorbent was done by adopting strategies similar to earlier studies [42,43].

2.2. Preparation of the adsorbent ash

In the dye removal study, ash of *C. caesia* was used as adsorbent. Fresh Bluish black rhizome of *C. caesia* was procured from Kandhamal, Odisha, India. The collected rhizomes were sun-dried and powdered. The powdered rhizomes were converted into ash by heating in a muffle furnace at 550°C for 5 h. After cooling, the ash is collected and used without any chemical treatment.

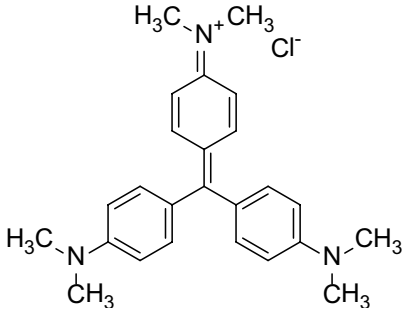

Fig. 1. Chemical structure of crystal violet dye.

2.3. Dye adsorption study via batch technique

Batch adsorption experiments were carried out with 10 mL CV dye solution for 3–8 mg/L initial dye concentrations, 5–30 mg of adsorbent, 4–9 pH, 1–24 h contact time, and 25°C–45°C temperature. pH of dye solution was adjusted by adding dilute solutions of HCl and NaOH. Dye concentration was analyzed spectrophotometrically by UV-vis spectrophotometer at maximum wavelength (λ_{max}) 589 nm in absorbance mode. The removal efficiency (R, %), amount of dye adsorbed at time t (Q_t, mg/g), and amount of dye adsorbed at equilibrium (Q_e, mg/g) were calculated using the reported formulas [44].

2.4. Adsorption equilibrium

Equilibrium experiments were performed in 10 mL dye solutions of different initial concentrations (3–8 mg/L) mixed with 0.01 g of adsorbent. 24 h is considered as an equilibrium time. After 24 h samples were analyzed as mentioned earlier.

2.5. Adsorption kinetics

Experiments for adsorption kinetic study were carried out by adding 0.01 g of adsorbent with 10 mL aqueous solution of CV dye having 8 mg/L initial dye concentrations. The remaining dye concentrations in the samples were recorded at different time intervals as described earlier.

2.6. Dye adsorption study via column run technique

For column adsorption, 0.5 g ash of *C. caesia* adsorbent was filled in a glass column to make a fixed bed of 1.3 cm height and 0.2 cm^2 cross-sectional area. The glass column has 0.5 cm internal diameter and 19 cm length. Through this fixed bed aqueous solution of CV dye having 5 mg/L initial dye concentration was allowed to run in a down flow motion with a flow rate of 1.3 mL/min and after each 5 min time interval, 6.5 mL aqueous effluent samples were collected and dye concentration was determined by measuring characteristics absorbance of the dye. The dynamic behavior of column is explained by breakthrough curve [19,35] which is obtained by plotting a graph of normalized concentration, ratio of effluent dye concentration at time t to initial dye concentration (C_t/C_0), vs. time. Breakthrough parameters, that is, total amount of dye (m_{total}) passed through the column at time t, percentage removal of dye R(%), and column adsorption capacity of the adsorbent q_t (mg/g) at time t were calculated using the reported formulas [19,35].

Column studies differ to the batch studies in a way that in column operations adsorbent remains continuously in contact with the solution of the adsorbate as a result of which the concentration of the adsorbate solution remains constant throughout its contact with the adsorbent. However, in case of batch operations the concentration of the adsorbate, which is in contact with the adsorbent, decreases gradually during adsorption. Therefore, due to gradual adsorption of the adsorbate over the surface of adsorbent effectiveness of the adsorbent drops off with time. Thus, in the batch adsorption the time required for the adsorbent and adsorbate to attain substantial equilibrium is large and additional time is required for the filtration process. Because of these limitations batch reactors do not give precise data and the practical applicability of the use of the adsorbent materials is ascertained through column operations [45–48]. It is also observed that the exhaustion capacity in the fixed bed operations is relatively higher, indicating thereby better efficiency of column operations than the batch removal [49,50]. This is due to formation of continuous larger concentration gradient at the interface zone as the influent dye solution passes through the column. Moreover, fixed bed column operations are simple to operate, can be scaled-up from a laboratory process and effects of adsorbent recycling ability can be judged through this method [51]. Because of these reasons continuous adsorption in fixed-bed column is often desired from industrial point of view. In the present studies, continuous flow system in which the adsorbent is continuously in contact with fresh solution of adsorbate is used and column is prepared as described in several other studies [52,53].

3. Result and discussion

3.1. Characterization of adsorbent

Scanning electron micrographs of *C. caesia* ash before and after CV dye adsorption are shown in Figs. 2a and 2b, respectively. Fig. 2a reveals the presence of porous texture in the surface of the adsorbent and adsorption of CV dye at the ash surface is confirmed by the coverage of ash surface depicted in Fig. 2b. Change in IR peaks of the ash adsorbent before and after adsorption (Figs. S1 and S2) also confirms the adsorption process. IR peaks of *C. caesia* ash were observed at 1,397.33 and 1,007.13 cm^{-1} before adsorption of dye which was shifted to 1,012.62 cm^{-1} after adsorption of crystal violet. The observation indicates formation of chemical bond in the course of adsorption. X-ray diffraction (XRD) pattern of the adsorbent is shown in Fig. S3 which reveals the peaks at 2θ angles 26.7°, 28.6°, 30.5°, 32.8°, 34.1°, 40.64°, 43.4°, and 45.1°. XRD pattern was found to remain unchanged (after desorption) after every cycle till eighth cycles.

3.2. Effect of initial dye concentration and contact time

On increasing initial dye concentration, an increase in removal efficiency of CV dye is found as shown in Fig. 3 which may be probably due to increase in the mass gradient between the dye solution and adsorbent ash as the initial dye concentration increases [54]. Further, Fig. 3 also reveals increase in the removal of CV dye with increasing contact time.

3.3. Effect of adsorbent dose

Fig. 4 shows the effect of amount of adsorbent ash of *C. caesia* on CV dye removal and it is observed that the removal of CV dye removal increases as the amount of the adsorbent is increased from 5 to 30 mg. This can be attributed with the increase in the surface area and adsorption sites on increasing amount of adsorbent [55]. 99.95% dye removal has been observed at 30 mg dose of adsorbent.

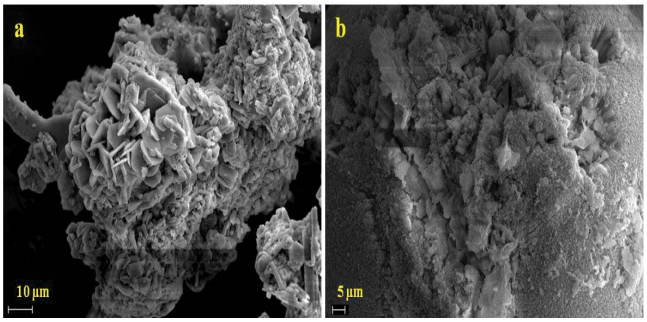

Fig. 2. SEM micrographs of *Curcuma caesia* ash (a) before and (b) after adsorption of CV dye.

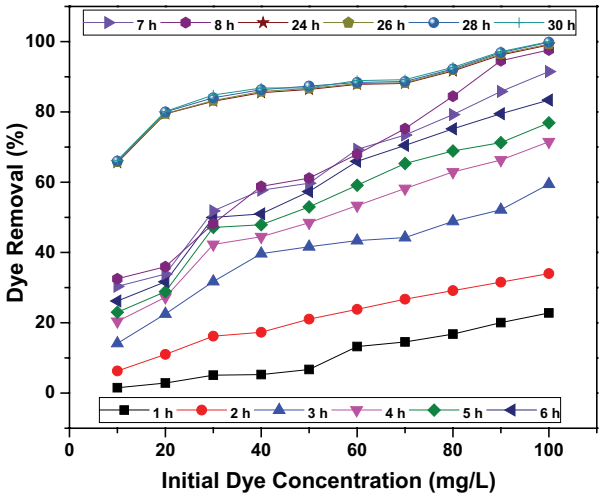

Fig. 3. Effect of initial dye concentration and contact time.

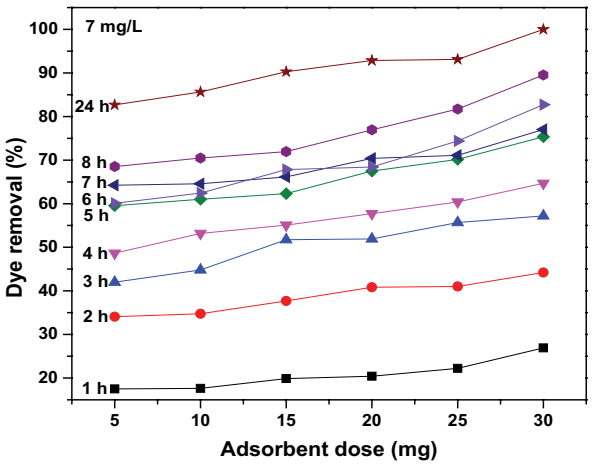

Fig. 4. Effect of adsorbent dose on removal of crystal violet dye.

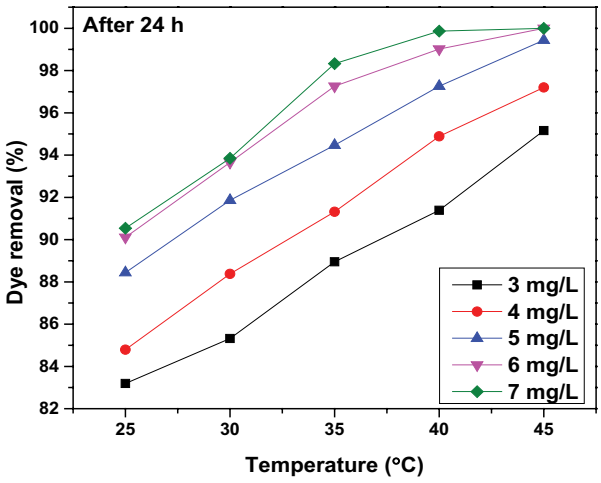

Fig. 5. Effect of temperature on removal of crystal violet dye.

3.4. Effect of temperature

Effect of temperature on removal of CV dye was studied at different temperatures viz., 25°C, 30°C, 35°C, 40°C, and 45°C and the results obtained are presented in Fig. 5. Here, amount of adsorbent (*C. caesia ash*) was taken 15 mg at all temperatures. The removal of dye from its aqueous solution increases with increasing temperature, revealing the endothermic nature of adsorption process, and increase in mobility of dye molecules with increase in temperature [54,56].

3.5. Effect of pH of dye solution

pH of the CV dye solution was adjusted in the range between pH 4 and 9 to study the effect of pH of dye solution on dye removal and here, the amount of adsorbent (*C. caesia* ash) was taken 15 mg at all pH 4–9. The obtained experimental data indicated that the CV dye removal was more effective at higher pH as shown in Fig. 6a. This behavior of adsorbent on different pH can be explained on the basis of protonation and deprotonation of CV dye in acidic and basic mediums, respectively. At lower pH, presence of excess H^+ ions makes dye molecules highly positive charged, suggesting the existence of repulsion between positively charged surface and the positively charged dye molecules. Therefore, lower adsorption of dye molecules. On the other hand, in the basic medium the formation of electric double layer changes its polarity and consequently the dye uptake increases [21,57].

On the other hand, effect of initial pH of dye solution can be explained by surface charge of the adsorbent which was determined by zeta potential. As shown in Fig. 6b, the adsorbent has positive zeta potential at lower pH indicating the positive surface charge which turns negative as the pH increases. In higher pH ranges the adsorbent surface carries negative charge which benefits the adsorption of cationic CV dye through electrostatic interaction. Therefore, adsorption rate were improved with increasing pH values [58,59].

3.6. Adsorption isotherm study

To explain the interaction behavior of CV dye molecules with the adsorbent and distribution of dye molecules between the two phases, that is, solid phase and liquid

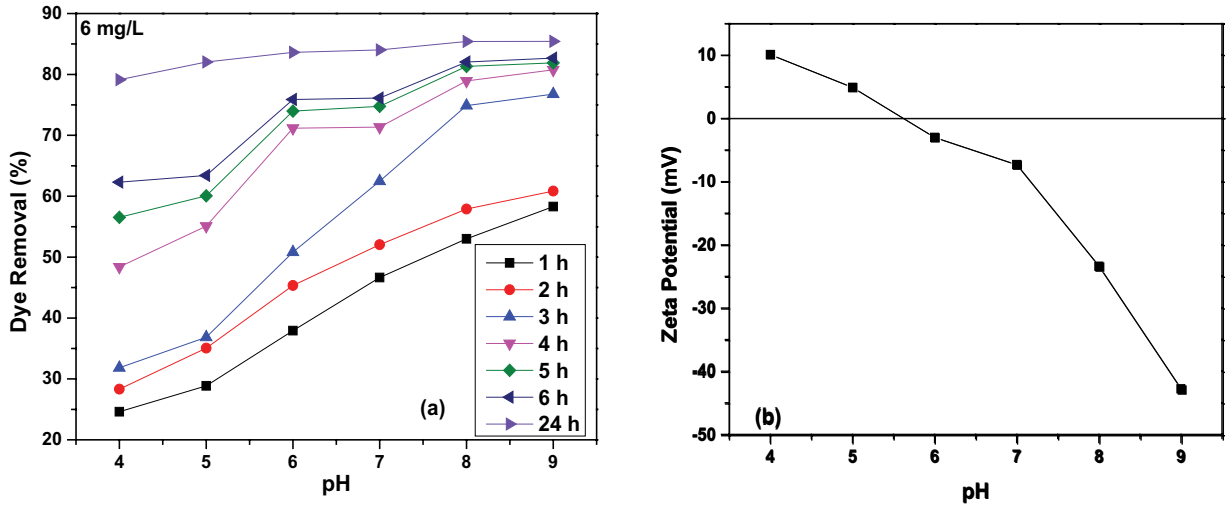

Fig. 6. (a) Effect of pH on removal of crystal violet dye and (b) zeta potential of ash of *Curcuma caesia* ash.

phase, three adsorption isotherm models viz., Freundlich, Langmuir, and Temkin isotherm model were applied and linear equations of these three isotherm models are given as following Eqs. (1)–(3), respectively.

Freundlich adsorption isotherm:

$$\ln Q_e = \ln K_f + \frac{1}{n}\ln C_e \tag{1}$$

Langmuir adsorption isotherm:

$$\frac{C_e}{Q_e} = \frac{C_e}{Q_L} + \frac{1}{K_L Q_L} \tag{2}$$

Temkin adsorption isotherm:

$$Q_e = \frac{RT}{b_T}\ln C_e + \frac{RT}{b_T}\ln K_T \tag{3}$$

Here, C_e is the equilibrium concentration (mg/L) of CV dye solution, Q_e is the adsorption capacity (mg/g). Freundlich model explains adsorption on the heterogeneous surface with non-uniform distribution of heat of adsorption. It assumes that there is an interaction between adsorbed molecules [55,58]. Freundlich constants K_f and n are related to the adsorption capacity and adsorption intensity, respectively. Value of constant n provides the information about how favorable is the adsorption process. If the value of $1/n$ is closer to 0, adsorption becomes more heterogeneous [59].

Langmuir isotherm takes into account the monolayer adsorption of dye molecules onto homogeneous surface of adsorbent without any interaction between the adsorbed dye molecules. K_L and Q_L are the Langmuir constant related to rate of adsorption and adsorption capacity, respectively [56,60,61].

According to Temkin isotherm, there is a linear increase in the heat of adsorption of all the molecules with coverage of adsorbate over adsorbent surface. The Temkin isotherm constants (b_T and K_T) can be calculated from slope and intercept of the plot of $\ln C_e$ vs. Q_e. K_T is the equilibrium binding constant (L/mg) corresponding to the maximum binding energy and constant b_T is related to the heat of adsorption [32].

Plots for the above three adsorption isotherm models were drawn using the experimental data (Figs. 7–9) and their corresponding constants are listed in Table 1. From Table 1, the Temkin isotherm model revealed the best fit with highest R^2 value (0.96933) compared to the other two models. This indicates the presence the energetically non-equivalent adsorption sites on the surface of adsorbent and the adsorption of CV takes place on the more energetic adsorption site at first [61].

3.7. Kinetic study

In order to interpret the experimental data of adsorption process, three kinetic models Lagergren's pseudo-first-order model, Ho's pseudo-second-order model, and Weber and Morris' intraparticle diffusion model were applied whose liner forms can be expressed as given in Eqs. (4)–(6) [62,63].

Pseudo-first-order kinetics:

$$\ln\left(Q_e - Q_t\right) = \ln Q_e - k_1 t \tag{4}$$

Pseudo-second-order kinetics:

$$\frac{t}{Q_t} = \frac{t}{Q_e} + \frac{1}{k_2 Q_e^2} \tag{5}$$

Intraparticle diffusion:

$$Q_t = k_i t^{1/2} + C \tag{6}$$

Here, Q_e (mg/g) and Q_t (mg/g) are the amount of dye adsorbed at equilibrium and at time t (min), respectively,

and k_1 (min^{-1}), k_2 (g/mg min), k_i (mg/g min$^{1/2}$) are rate constant of adsorption for pseudo-first-order, pseudo-second-order, and intraparticle diffusion respectively. In intraparticle diffusion constant C reflects the boundary layer effect [62].

Three linear plots for the kinetic models are presented in Figs. 10–12 and their corresponding parameters are listed in Table 2. The value of R^2 (0.989) for pseudo-second-order kinetics is closer to unity and is greater than that of the two other kinetic models. This suggests that the pseudo-second-order kinetic model with rate constant 1.85×10^{-4} g/mg min is best fit for the present study which indicates the CV dye was removed from its aqueous solution via chemisorptions process [19]. Further, the calculated uptake capacity (Q_e^{cal} = 23.753 mg/g) is in good agreement with the experimental uptake capacity (Q_e^{exp} = 20.809 mg/g).

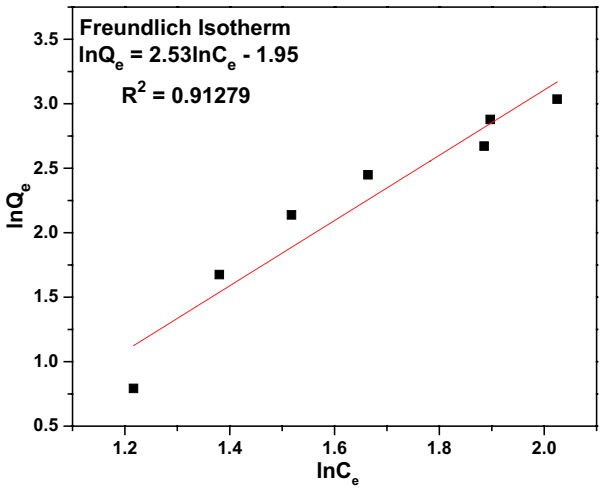

Fig. 7. Linear plot for Freundlich adsorption isotherm.

3.8. Determination of thermodynamic parameters

To determine the thermodynamic parameters, that is, enthalpy (H), entropy (S), and free energy (G) for the present study following Eqs. (7) and (8) were used:

$$\ln\frac{Q_e m}{C_e} = \frac{\Delta S}{R} - \frac{\Delta H}{RT} \tag{7}$$

$$\Delta G = \Delta H - T\Delta S \tag{8}$$

where, ΔS, ΔH, and ΔG are the change in entropy (kJ/mol/K), enthalpy (kJ/mol), and Gibb's free energy (kJ/mol), respectively. m is the adsorbent dose (g/L), C_e is the equilibrium concentration (mg/L) of dye solution, Q_e is the

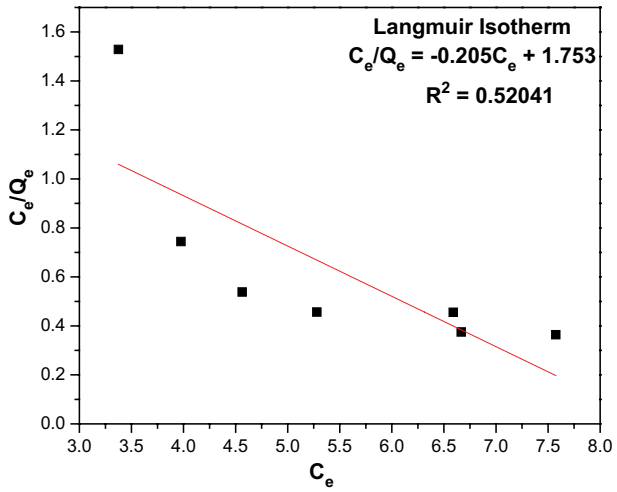

Fig. 8. Linear plot for Langmuir adsorption isotherm.

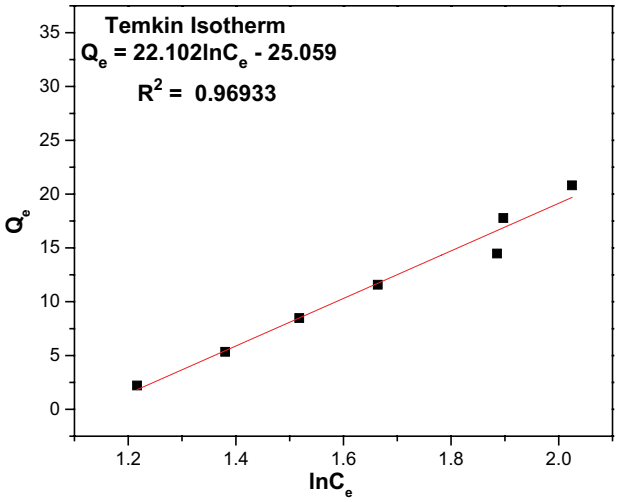

Fig. 9. Linear plot for Temkin adsorption isotherm.

Table 1
Adsorption isotherm parameters for adsorption of crystal violet dye on *Curcuma caesia* ash

S. No.	Adsorption isotherms	Parameters	R^2
1	Freundlich adsorption isotherm	n = 0.395 (1/n = 2.532) K_f = 0.142 mg/g	0.91279
2	Langmuir adsorption isotherm	K_L = –0.117 mg/g Q_L = –4.878 mg/g	0.52041
3	Temkin adsorption isotherm	b_T = 113.978 J/mol K_T = 0.322 L/mol	0.96933

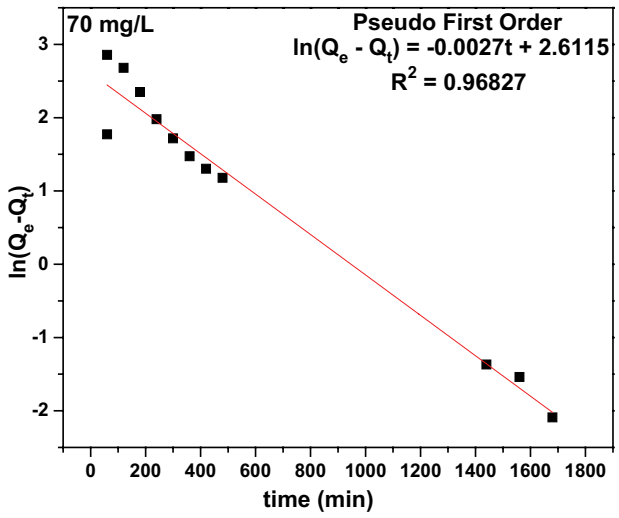

Fig. 10. Linear plot for pseudo-first-order kinetic model.

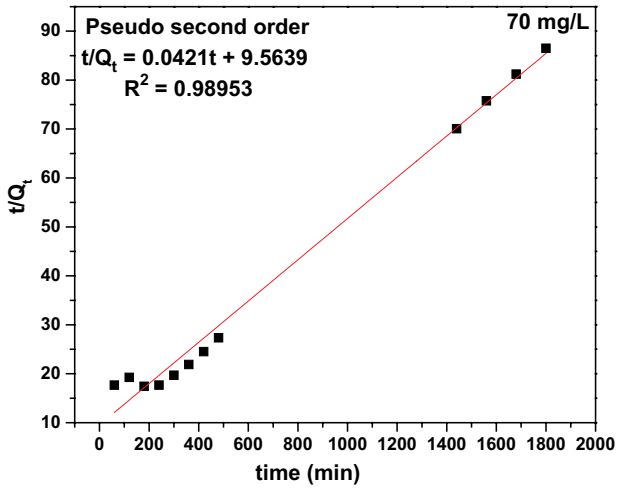

Fig. 11. Linear plot for pseudo-second-order kinetic model.

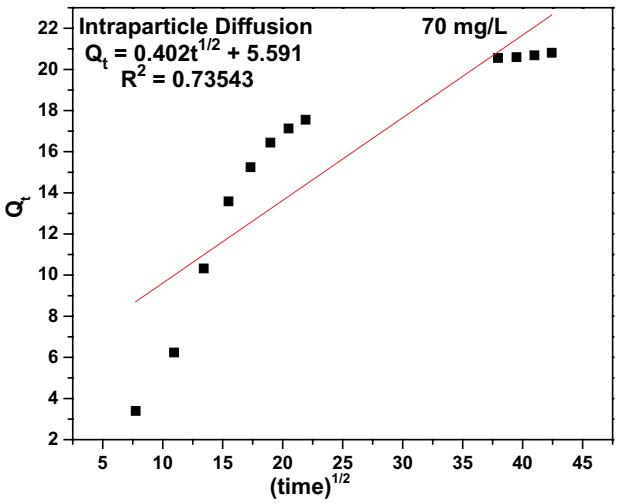

Fig. 12. Linear plot for intraparticle diffusion kinetic model.

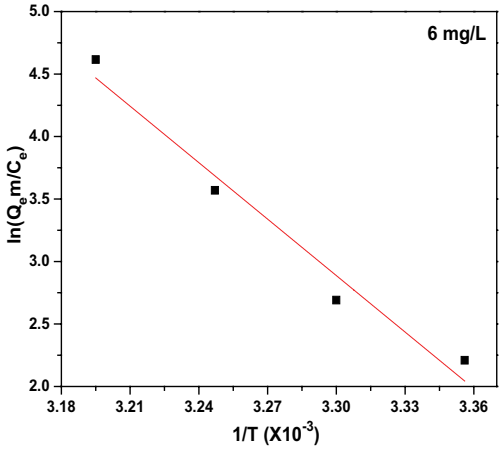

Fig. 13. Plot of $\ln(Q_e m/C_e)$ vs. $1/T$ to give thermodynamic parameters.

amount of dye adsorbed at equilibrium (mg/g), R is the gas constant (8.314 J/mol/K), and T is temperature (K).

The values of ΔH and ΔS were calculated using the slop ($\Delta H/R$) and intercept ($\Delta S/R$) of a linear plot which is drawn between $\ln(Q_e m/C_e)$ and $1/T$ as shown in Fig. 13 and the values of ΔG at different temperatures were calculated using Eq. (8). The values of thermodynamic parameters obtained are presented in Table 3. The feasibility of the adsorption process and its spontaneous nature is confirmed by the negative values of free energy [64]. Further, the increase in absolute value of free energy ΔG with temperature indicates that the adsorption is favorable at higher temperature [65]. The positive ΔH value confirms the endothermic nature of the adsorption. Positive value of ΔS indicates an increase in randomness at the solid-solution interface during the adsorption process [65].

3.9. Column adsorption study of CV dye removal on black turmeric ash

Column operation was carried out to check the practical usability of the adsorbent. To analyze the column efficiency

Table 2
Kinetic parameters for adsorption of crystal violet dye on *Curcuma caesia* ash

	Pseudo-first-order			Pseudo-second-order			Intraparticle diffusion		
Q_e^{exp} (mg/g)	Q_e^{cal}	k_1	R^2	Q_e^{cal}	k_2	R^2	k_i	C	R^2
20.809	13.619	0.003	0.968	23.753	0.0001853	0.989	0.402	5.591	0.735

Table 3
Thermodynamic parameters for CV adsorption on *Curcuma caesia* ash

ΔH (kJ/mol)	ΔS (kJ/mol/K)	ΔG (kJ/mol) at temperatures				
		298 K	303 K	308 K	313 K	318 K
125.26	0.44	–5.07	–7.26	–9.44	–11.63	–13.82

Table 4
Breakthrough parameters for column adsorption study of CV dye using *Curcuma caesia* ash

Flow rate (mL/min)	Time (min)	Peak area (mg min/L)	Column adsorption capacity (mg/g)	Amount of dye passed through the column (mg)	Amount of dye adsorbed by the column (mg)	Percentage removal of dye (%)
1.3	355	1,370.58	3.56	2.31	1.78	77.06

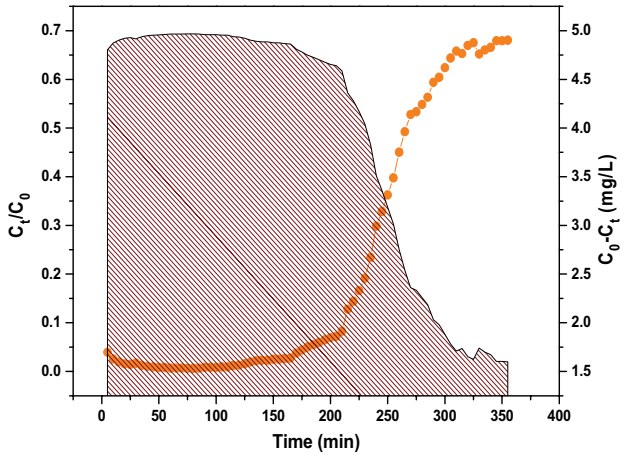

Fig. 14. Breakthrough curve (line, left vertical axis) and integral area (oblique line, right vertical axis) of crystal violet dye on ash of *Curcuma caesia* fixed bed column.

of an adsorbent breakthrough curve is used which is plotted between C_t/C_0 and time. The breakthrough curve and its integral area (drawn by software OriginPro 8) are shown in Fig. 14. The calculated breakthrough parameters are shown in Table 4. According to integral area, the calculated column adsorption capacity was found to be 3.56 mg/g which is relatively lower than the batch adsorption capacity.

4. Conclusion

Crystal violet dye was successfully removed from its aqueous solutions by using natural adsorbent black turmeric and the influences of several factors affecting the adsorption process were studied. The adsorption was found to be endothermic in nature and favored in basic medium (pH 9). Complete removal of dye was achieved at 40°C and above. 99.95% dye removal was observed at 30 h at adsorbent dose of 30 mg. The adsorption process for dye removal was controlled by pseudo-second-order kinetics with rate constant 1.85×10^{-4} g/mg min and Temkin adsorption isotherm. The endothermic nature of the process was also confirmed by the thermodynamic parameters. Thermodynamic parameters also revealed the feasibility and spontaneous nature along with the favorability at higher temperatures. For the present study, the column adsorption capacity was lower than the batch adsorption capacity. The calculated uptake capacity (Q_e^{cal} = 23.753 mg/g) was found in good agreement with the experimental uptake capacity (Q_e^{exp} = 20.809 mg/g).

References

[1] F.M.D. Chequer, D.J. Dorta, D. Palma de Oliveira, Azo Dyes and Their Metabolites: Does the Discharge of the Azo Dye into Water Bodies Represent Human and Ecological Risks, P.J. Hauser, Ed., Advances in Treating Textile Effluent, 2011, InTechOpen. Available at: https://www.intechopen.com/books/advances-in-treating-textile-effluent/azo-dyes-and-their-metabolites-does-the-discharge-of-the-azo-dye-into-water-bodies-represent-human-a
[2] R.D. Saini, Textile organic dyes: polluting effects and elimination methods from textile waste water, Int. J. Chem. Eng. Res., 9 (2017) 121–136.
[3] Y. Anjaneyulu, N. Sreedhara Chary, D.S. Suman Raj, Decolourization of industrial effluents – available methods and emerging technologies – a review, Rev. Environ. Sci. Biotechnol., 4 (2005) 245–273.
[4] P. Nigam, G. Armou, I.M. Banat, D. Singh, R. Marchant, Physical removal of textile dyes and solid-state fermentation of dye-adsorbed agricultural residues, Bioresour. Technol., 72 (2000) 219–226.
[5] P. Pengthamkeerati, T. Satapanajaru, N. Chatasatapattayakul, P. Chairattanamanokom, N. Sananwai, Alkaline treatment of biomass fly ash for reactive dye removal from aqueous solution, Desalination, 261 (2010) 34–40.
[6] M. Mobarak, E.A. Mohamed, A.Q. Selim, M.F. Eissa, M.K. Seliem, Experimental results and theoretical statistical modelling of malachite green adsorption onto MCM-41 silica/rice husk composite modified by beta radiation, J. Mol. Liq., 273 (2019) 68–82.
[7] S. De Gisi, G. Lofrano, M. Grassi, M. Notarnicola, Characteristics and adsorption capacities of low-cost sorbents foe waste water treatment: a review, Sustainable Mater. Technol., 9 (2016) 10–40.
[8] K.D. Zhang, F.C. Tsai, N. Ma, Y. Xia, H.L. Liu, X.Q. Zhan, X.Y. Yu, X.Z. Zeng, T. Jiang, D. Shi, C.J. Chang, Adsorption behavior of high stable Zr-based MOFs for the removal of acid organic dye from water, Materials, 10 (2017) 205, doi: 10.3390/ma10020205.
[9] A. Mohamed, S. Yousef, M.A. Abdelnaby, T. Osman, B. Hamawandi, M. Toprak, M. Muhammed, A. Uheida, Photocatalytic degradation of organic dyes and enhanced mechanical

properties of PAN/CNTs composite nanofibers, Sep. Purif. Technol., 182 (2017) 219–223.
[10] S. Kuriakose, B. Satpati, S. Mohapatra, Highly efficient photocatalytic degradation of organic dyes by Cu doped ZnO nanostructures, Phys. Chem. Chem. Phys., 17 (2015) 25172–25181.
[11] M. Pourgholi, R.M. Jahandizi, M. Miranzadeh, O.H. Beigi, S. Dehghan, Removal of dye and COD from textile wastewater using AOP (UV/O_3, UV/H_2O_2, O_3/H_2O_2 and $UV/H_2O_2/O_3$), J. Environ. Health Sustainable Dev., 3 (2018) 630–636.
[12] V.K. Gupta, R. Jain, A. Mittal, T.A. Saleh. A. Nayak, S. Agarwal, S. Sikarwar, Photo-catalytic degradation of toxic dye amaranth on TiO_2/UV in aqueous suspensions, Mater. Sci. Eng., C, 32 (2012) 12–17.
[13] V.K. Gupta, Suhas, Application of low-cost adsorbents for dye removal – a review, J. Environ. Manage., 90 (2009) 2313–2342.
[14] L. Bulgariu, L.B. Escudero, O.S. Bello, M. Iqbal, J. Nisar, K.A. Adegoke, F. Alakhras, M. Kornaros, I. Anastopoulos, The utilization of leaf-based adsorbents for dyes removal: a review, J. Mol. Liq., 276 (2019) 728–747.
[15] A. Kausar, M. Iqbal, A. Javed, K. Aftab, Z.-i.-H. Nazil, H.N. Bhatti, S. Nouren, Dye adsorption using clay and modified clay: a review, J. Mol. Liq., 256 (2018) 395–407.
[16] I. Anastopoulos, A. Hosseini-Bandegharaei, J. Fu, A.C. Mitropoulos, G.Z. Kyzas, Use of nanoparticles to dye adsorption: review, J. Dispersion Sci. Technol., 39 (2017) 836–847.
[17] A. Bhatnagar, M. Sillanpaa, A. Witek-Krowiak, Agricultural waste peels as versatile biomass for water purification – a review, Chem. Eng. J., 270 (2015) 244–271.
[18] I. Khurana, A. Saxena, Bharti, J.M. Khurana, P.K. Rai, Removal of dyes using graphene-based composites: a review, Water Air Soil Pollut., 228 (2017) 180, doi: 10.1007/s11270-017-3361-1.
[19] C. Arora, S. Soni, S. Sahu, J. Mittal, P. Kumar, P.K. Bajpai, Iron based metal organic framework for efficient removal of methylene blue dye from industrial waste, J. Mol. Liq., 284 (2019) 343–352.
[20] C. Arora, D. Sahu, D. Bharti, V. Tamrakar, S. Soni, S. Sharma, Adsorption of hazardous dye crystal violet from industrial waste using low cost adsorbent *Chenopodium album*, Desal. Water Treat., 167 (2019) 324–332.
[21] I.D. Mall, V.C. Srivastava, N.K. Agarwal, I.M. Mishra, Adsorptive removal of malachite green dye from aqueous solution by bagasse fly ash and activated carbon kinetic study and equilibrium isotherm analyses, Colloids Surf., A, 264 (2005) 17–28.
[22] M.M. Hasan, M.N. Hasan, M.R. Awual, M.M. Islam, Biodegradable natural carbohydrate polymeric sustainable adsorbents for efficient toxic dye removal from wastewater, J. Mol. Liq., 319 (2020) 1143562, doi: 10.1016/j.molliq.2020.114356.
[23] A.J. Khan, J. Song, K. Ahmed, A. Rahim, P.L.O. Volpe, Mesoporous silica MCM-41, SBA-15 and derived bridged polysilsesquioxane SBA-PMDA for the selective removal of textile reactive dyes from wastewater, J. Mol. Liq., 298 (2020) 111957, doi: 10.1016/j.molliq.2019.111957.
[24] N. Marsiezade, V. Javanbakht, Novel hollow beads of carboxymethyl cellulose/ZSM-5/ZIF-8 for dye removal from aqueous solution in batch and continuous fixed bed systems, Int. J. Biol. Macromol., 162 (2020) 1140–1152.
[25] S.I. Siddiqui, F. Zohra, S.A. Chaudhry, *Nigella sativa* seed based nanohybrid composite-Fe_2O_3–SnO_2/BC: a novel material for enhanced adsorptive removal of methylene blue from water, Environ. Res., 178 (2019) 1086672, doi: 10.1016/j.envres.2019.108667.
[26] W. Astuti, A. Chafidz, E.T. Wahyuni, A. Prasetya, Methyl violet dye removal using coal fly ash (CFA) as a dual sites adsorbent, J. Environ. Chem. Eng., 7 (2019), doi: 10.1016/j.jece.2019.103262.
[27] X. Yao, Y. Zheng, H. Zhou, K. Xu, Q. Xu, L. Li, Effects of biomass blending, ashing temperature and potassium addition on ash sintering behaviour during co-firing of pine sawdust with a Chinese anthracite, Renewable Energy, 147 (2020) 2309–2320.
[28] X. Yao, H. Zhou, K. Xu, S. Chen, J. Ge, Q. Xu, Systematic study on ash transformation behaviour and thermal kinetic characteristics during co-firing of biomass with high ratios of bituminous coal, Renewable Energy, 147 (2020) 1453–1468.
[29] X. Yao, H. Zhou, K. Xu, Q. Xu, L. Li, Evaluation of the fusion and agglomeration properties of ashes from combustion of biomass, coal and their mixtures and the effects of K_2CO_3 additives, Fuel, 255 (2019) 11829–11840.
[30] V. Tamrakar, C. Arora, *Curcuma caesia*: present status and future prospect as herbal drug, Prog. Agric., 23 (2019) 113–117.
[31] K.V. Roopavathi, S. Shanthakumar, Adsorption capacity of *Curcuma longa* for the removal of basic green 1 dye - equilibrium, kinetics and thermodynamic study, J. Environ. Biol., 37 (2016) 979–984.
[32] A. Mittal, J. Mittal, A. Malviya, D. Kaur, V.K. Gupta, Adsorption of hazardous dye crystal violet from waste water by waste materials, J. Colloid Interface Sci., 343 (2010) 463–473.
[33] A.L. Prasad, T. Santhi, Adsorption of hazardous cationic dyes from aqueous solution onto *Acacia nilotica* leaves as an eco friendly adsorbent, Sustainable Environ. Res., 22 (2012) 113–122.
[34] S. Senthilkumar, P. Kalaamani, C.V. Subburaam, Liquid phase adsorption of crystal violet onto activated carbons derived from male flowers of coconut tree, J. Hazard. Mater., 136 (2006) 800–808.
[35] J.X. Yu, J. Zhu, L.Y. Feng, X.L. Cai, Y.F. Zhang, R.A. Chi, Removal of cationic dyes by modified waste biosorbent under continuous model: competitive adsorption and kinetics, Arabian J. Chem., 12 (2019) 2044–2051.
[36] A.K. Jain, V.K. Gupta, A. Bhatnagar, Suhas, Utilization of industrial waste products as adsorbents for the removal of dyes, J. Hazard. Mater., 101 (2003) 31–42.
[37] A.K. Jain, V.K. Gupta, A. Bhatnagar, S. Jain, Suhas, A comparative assessment of adsorbents prepared from industrial wastes for the removal of cationic dye, J. Indian Chem. Soc., 80 (2003) 267–270.
[38] J. Song, W. Zou, Y. Bian, F. Su, R. Han, Adsorption characteristics of methylene blue by peanut husk in batch and column modes, Desalination, 265 (2011) 119–125.
[39] W.J. Weber, Physicochemical Processes for Quality Control, Wiley-Interscience, New York, NY, 1972.
[40] K.I. Anderson, M. Erikson, M. Norgen, Lignin removal by adsorption to fly ash in wastewater generated by mechanical pulping, Ind. Eng. Chem. Res., 51 (2012) 3444–3451.
[41] C. Arora, S. Bhattacharya, S. Soni, P. Maji, Scanning Electron Microscopy: Theory and Applications, Y. Tutar, Ed., Essential Techniques for Medical and Life Scientists: A Guide to Contemporary Methods and Current Applications With the Protocols: Part 2, Bentham Science Publishers, Singapore, 2020, pp. 117–123.
[42] Y. Fu, L. Qin, D. Huang, G. Zeng, C. Lai, B. Li, J. He, H. Yi, M. Zhang, M. Cheng, X. Wen, Chitosan functionalized activated coke for Au nanoparticles anchoring: green synthesis and catalytic activities in hydrogenation of nitrophenols and azo dyes, Appl. Catal., B, 255 (2019) 117740–117746.
[43] L. Qin, Z. Zeng, G. Zeng, C. Lai, A. Duan, R. Xiao, D. Huanga, Y. Fu, H. Yi, B. Li, X. Liu, S. Liu, M. Zhang, D. Jiang, Cooperative catalytic performance of bimetallic Ni-Au nanocatalyst for highly efficient hydrogenation of nitroaromatics and corresponding mechanism insight, Appl. Catal., B, 259 (2019), doi: 10.1016/j.apcatb.2019.118035.
[44] S. Soni, P.K. Bajpai, J. Mittal, C. Arora, Utilisation of cobalt doped iron based MOF for enhanced removal and recovery of methylene blue dye from waste water, J. Mol. Liq., 284 (2020) 343–352.
[45] S.S. Baral, N. Das, T.S. Ramulu, S.K. Sahoo, S.N. Das, G.R. Chaudhury, Removal of Cr(VI) by thermally activated weed *Salvinia cucullata* in a fixed–bed column, J. Hazard. Mater., 161 (2009) 1427–1435.
[46] A. Olgun, N. Atar, Equilibrium and kinetic adsorption study of Basic Yellow 28 and Basic Red 46 by a boron industry waste, J. Hazard. Mater., 161 (2009) 148–156.
[47] L. Monse, N. Adhoum, Tartrazine modified activated carbon for the removal of Pb(II), Cd(II) and Cr(III), J. Hazard. Mater., 161 (2009) 263–269.
[48] P. Suksabye, P. Thiravetyan, W. Nakbanpote, Column study of Chromium(VI) adsorption from electroplating industry by coconut coir pith, J. Hazard. Mater., 160 (2008) 56–62.

[49] G. Bayramoglu, G. Celik, M.Y. Arica, Biosorption of Reactive Blue 4 dye by native and treated fungus *Phanerocheate chrysosporium*: batch and continuous flow system studies, J. Hazard. Mater., 137 (2006) 1689–1697.
[50] A. Mittal, J. Mittal, L. Kurup, Batch and bulk removal of hazardous dye, Indigo carmine from wastewater through adsorption, J. Hazard. Mater., 137 (2006) 591–602.
[51] J.M. Chernand, Y.W. Chien, Adsorption of nitro phenol onto activated carbon: isotherms and breakthrough curves, Water Res., 36 (2002) 647–655.
[52] A.S. Michaels, Breakthrough curves in ion–exchange, Ind. Eng. Chem., 44 (1952) 1922–1930.
[53] W.A. Johnston, Designing fixed bed adsorbers, Chem. Eng., 79 (1972) 87–92.
[54] T.W. Seow, C.K. Lim, Removal of dye by adsorption: a review, Int. J. Appl. Eng. Res., 11 (2016) 2675–2679.
[55] A. Mittal, J. Mittal, A. Malviya, V.K. Gupta, Removal and recovery of chrysoidine Y from aqueous solutions by waste materials, J. Colloid Interface Sci., 344 (2010) 497–507.
[56] B.H. Hameed, A.A. Ahmad, Batch adsorption of methylene blue from aqueous solution by garlic peel, an agricultural waste biomass, J. Hazard. Mater., 164 (2009) 870–875.
[57] C. Arora, P. Kumar, S. Soni, J. Mittal, A. Mittal, B. Singh, Efficient removal of malachite green dye from aqueous solution using *Curcuma caesia* based activated carbon, Desal. Water Treat., 195 (2020) 341–352.
[58] P. Qin, Y. Yang, X. Zhang, J. Niu, H. Yang, S. Tian, J. Zhu, M. Lu, Highly efficient, rapid and simultaneous removal of cationic dyes from aqueous solution using monodispersed mesoporous silica nanoparticles as the adsorbent, Nanomaterials, 8 (2018), doi: 10.3390/nano801004.
[59] Y. Han, M. Liu, K. Li, Q. Sun, W. Zhang, C. Song, G. Zhang, Z.C. Zhang, X. Guo, *In situ* synthesis of titanium doped hybrid metal-organic framework UiO-66 with enhanced adsorption capacity for organic dyes, Inorg. Chem. Front., 4 (2017) 1870–1880.
[60] A. Mittal, J. Mittal, A. Malviya, D. Kaur, V.K. Gupta, Decoloration treatment of a hazardous triarylmethane dye, light green SF (yellowish) by waste material adsorbents, J. Colloid Interface Sci., 342 (2010) 518–527.
[61] Y. Xu, J. Jin, X. Li, Y. Han, H. Meng, C. Song, X. Zhang, Magnetization of a Cu(II)-1,3,5-benzenetricarboxylate metal-organic framework for efficient solid phase extraction of congo red, Microchim. Acta, 182 (2015) 2313–2320.
[62] B.S. Kaith, J. Sharma, Sukriti, S. Sethi, T. Kaur, U. Shankar, V. Jassal, Fabrication of green device for efficient capture of toxic methylene blue from industrial effluent based on $K_2Zn_3[Fe(CN)_6]_2{\cdot}9H_2O$ nanoparticles reinforced gum xanthan-psyllium hydrogel nanocomposite, J. Chin. Adv. Mater. Soc., 4 (2016) 249–268.
[63] A.K. Kushwaha, N. Gupta, M.C. Chattopadhyaya, Removal of cationic methylene blue and malachite green dyes from aqueous solution by waste materials of *Daucus carota*, J. Saudi Chem. Soc., 18 (2014) 200–207.
[64] R. Jain, S. Sikarwar, Photocatalytic and adsorption studies on the removal of dye congo red from wastewater, Int. J. Environ. Pollut., 27 (2006) 158–178.
[65] C. Li, X. Wang, D. Meng, L. Zhou, Facile synthesis of low cost magnetic biosorbent from peach gum polysaccharide for selective and efficient removal of cationic dyes, Int. J. Biol. Macromol., 107 (2018) 1871–1878.

Supplementary information

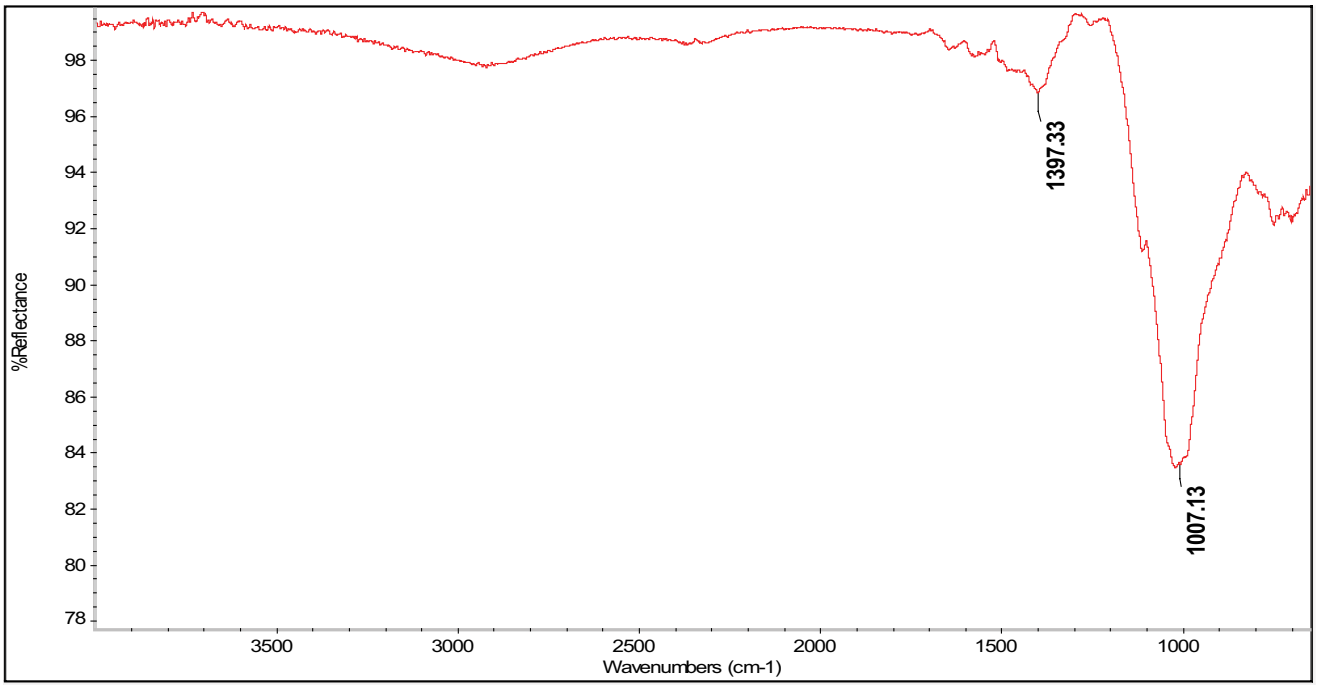

Fig. S1. IR spectra of *Curcuma caesia* ash before adsorption.

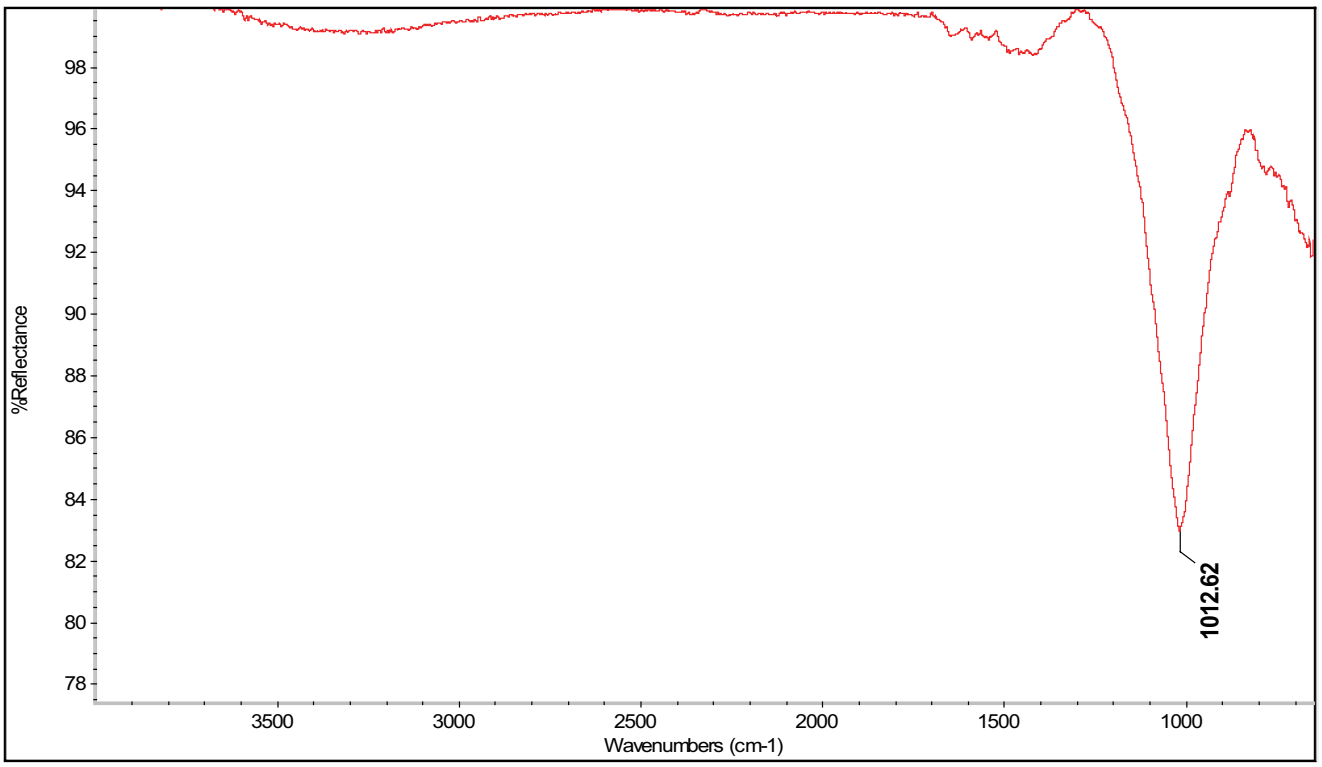

Fig. S2. IR spectra of *Curcuma caesia* ash after adsorption of CV dye.

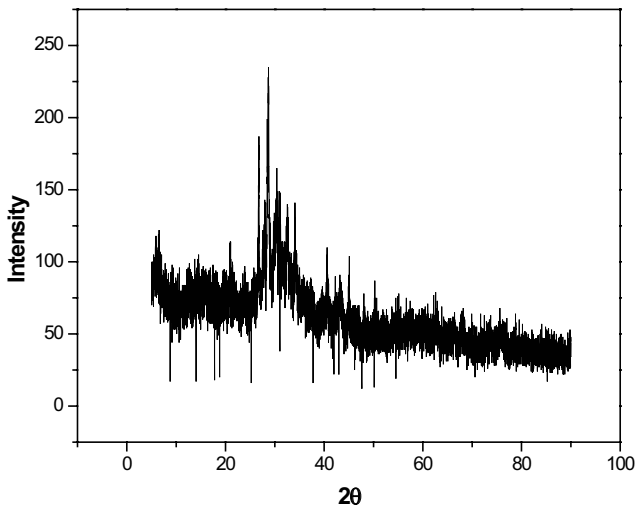

Fig. S3. PXRD pattern of ash of *Curcuma caesia*.